

## Multipole Analysis of X-Ray Diffraction Data on BeO

BY GENEVIÈVE VIDAL-VALAT AND JEAN PIERRE VIDAL

*Groupe de Dynamique des Phases Condensées (UA CNRS 233), Université des Sciences et Techniques du Languedoc, 34060 Montpellier CEDEX, France*

AND KAARLE KURKI-SUONIO AND RIITTA KURKI-SUONIO

*Department of Physics, University of Helsinki, SF-00170 Helsinki, Finland*

*(Received 23 July 1986; accepted 26 January 1987)*

### Abstract

X-ray diffraction intensities were measured from a BeO single crystal with wurtzite structure specially treated to reduce the extinction effects. Preliminary least-squares refinement yielded experimental structure factors on an absolute scale, corrected for extinction and anomalous dispersion, and a reference model  $\text{Be}^{2+}\text{O}^{2-}$  with the position parameter  $z = 0.3778$  (4) and anisotropic Debye-Waller factors corresponding to atomic mean-square displacements with spherical average  $\langle u^2 \rangle = 0.0045$  (3) and  $0.00353$  (1)  $\text{Å}^2$  and prolateness  $\langle u_3^2 \rangle - \langle u^2 \rangle = 0.0008$  (4) and  $0.00005$  (9)  $\text{Å}^2$  for  $\text{Be}^{2+}$  and  $\text{O}^{2-}$ , respectively. The residual differences  $F_o - F_c$  (of these experimental structure factors and those of the reference model) were analysed in terms of site-symmetrized multipole expansions. The phases of  $F_o$  were refined iteratively to take into account the effect of the significant multipole components found. The contribution of the  $\text{Be}^{2+}$  ion was subtracted to make possible a study of the oxygen lattice. Significant multipole components of third, fourth and sixth order indicate that the oxygen in BeO forms bonded hexagonal  $\text{O}^{2-}$  planes. They build up diffuse O–O bridges strongly bent towards the stabilizing  $\text{Be}^{2+}$  ions above the plane. The  $\text{Be}^{2+}$  ions exhibit a stretching quadrupole-like deformation suggesting some covalency of the bonding they build between the  $\text{O}^{2-}$  planes. There is some evidence of anharmonicity of atomic vibrations, particularly in the direction of the hexagonal axis.

### Introduction

This work completes our study of charge distributions of the alkaline-earth oxides. Beryllium oxide is the lightest in the series. Results on the heavier ones have been presented earlier by Vidal-Valat, Vidal & Kurki-Suonio (1978).

The experimental work on all these compounds was, in fact, done at the same time. The data on BeO were set aside because of problems in treating them in a comparable way. The extinction seemed worse and the method of analysis used was not applicable to it without further development.

The analysis of these data is, however, still motivated by the fact that, owing to experimental difficulties, no comparable data on BeO have been collected since then.

This work also presents the first application of "direct multipole analysis" on a non-centrosymmetric structure. Preliminary results of this work were presented at the Sagamore VII conference (Vidal, Vidal-Valat, Galtier & Kurki-Suonio, 1982).

BeO is an exceptional member in the series of alkaline-earth oxides. While the others are cubic with the NaCl structure BeO crystallizes in the polar space group  $P6_3mc$ . It has the wurtzite structure with two molecules in the hexagonal unit cell. The asymmetric unit consists of Be1 at  $\frac{1}{3}$ ,  $\frac{2}{3}$ , 0 and O1 at  $\frac{1}{3}$ ,  $\frac{2}{3}$ ,  $z$  both in special positions  $2(b)$  with site symmetry  $3m$ . The second molecule Be2, O2 is obtained from it through a  $60^\circ$  rotation around the hexagonal axis and the translation  $(\frac{1}{3}, -\frac{1}{3}, \frac{1}{2})$ .

Previous X-ray, neutron and  $\gamma$ -ray studies by Jeffrey, Parry & Mozzi (1956), Sabine & Dawson (1963), Smith, Newkirk & Kahn (1964), Pryor & Sabine (1964), Sabine & Hogg (1969), and Downs, Ross & Gibbs (1985) have given, consistently within experimental error,  $z = 0.378$  for the only structural parameter. Large extinction effects in BeO single crystals have been a problem. Anisotropic Debye-Waller values have been reported only with large uncertainty (Smith *et al.*, 1964). The main conclusions of these studies were that BeO is not completely ionic in character and that there are two different kinds of Be–O bonds, Be1–O2 and Be2–O1 being shorter and less ionic than Be1–O1 and Be2–O2, which are parallel to the hexagonal axis, (*cf.* Fig. 1).

The macroscopic physical properties of the alkaline-earth oxides vary in a systematic manner. For instance, the hardness, the elastic constants and the cohesive energy increase the hygroscopy and the polarizability and hence the relative permittivity decrease with decreasing cation atomic number (Huggins & Sakamoto, 1957; Julg, 1978; Miura, Murata & Shiro, 1978; Vempati & Jacobs, 1983). Apart from the systematic behaviour, the properties indicate the exceptional nature of BeO. In particular, BeO is not only harder than the other alkaline-earth oxides but it is among the hardest materials known. Its electrical conductivity is very low like that of the others, but its heat conductivity is an order of magnitude higher, which makes it a technically interesting ceramic (Kingery, Franch, Coble, & Vasilis, 1954; Campbell, 1956). It also possesses some interesting electret properties (Mucillo & Black, 1980).

The systematic behaviour of these properties have been related to the increasing covalent nature towards the lighter compounds of the series, which suggests further that BeO is clearly more covalent than the others. The anisotropy of the properties may give some indication of the differences in the nature of different bonds in BeO. It can be noted, for instance, that the static polarizability is clearly larger in the direction of the  $c$  axis while the anisotropy of its electronic contribution and hence the birefringence of the crystal is small (Smith, Newkirk & Kahn, 1964; Miura, Murata & Shiro, 1978).

The nature of bonding in BeO has been considered extensively in the context of lattice-dynamical studies. The anharmonicity of atomic vibrations in wurtzite-structure compounds has been studied with X-ray diffraction by Mair & Barnea (1975), Moss & Barnea (1976) and Whiteley, Moss & Barnea (1977, 1978). Isotropic Debye-Waller factors and dielectric constants derived from lattice-dynamical models of BeO based on a completely ionic character (Nusimovici, 1968; Hewat, 1972), were not in satisfactory agreement with the experimental values.

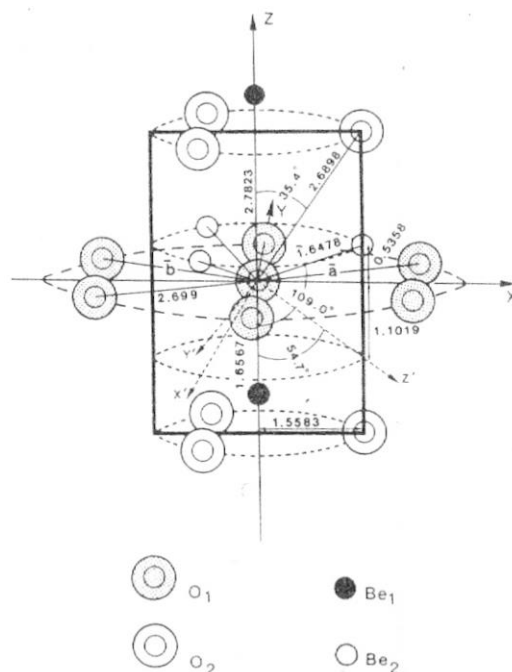


Fig. 1. The geometry of the surroundings of an oxygen atom in BeO with the local coordinate axes

Allowing for electronic expansion of ions in the model improved the agreement with observed macroscopic quantities but still revealed some incompatibilities (Miura, Murata & Shiro, 1977, 1978; Miura, Sat., Murata & Shiro, 1980). Inclusion of angular forces in the model led to a closer agreement (Rani, Gupta & Gupta, 1981).

Calculations of Hashimoto & Santry (1978) on BeO based on the CNDO method gave no converging results. The authors attributed this fact to an ionicity too strong for this method to be applicable. Momentum distributions derived from Compton scattering measurements of Fukamachi & Hosoya (1970) showed also large deviations from a completely ionic model of BeO, indicating the significance of solid-state effects inherent in the electronic state.

It is expected that accurate measurement of structure factors and a charge-density analysis based on them would shed some more light on the structural origin of the exceptional properties of BeO and on the nature of the problems met in their theoretical interpretation.

### Experimental procedures

The crystals were kindly provided by J. P. Mon (Département de Recherche de Physique, Paris). Preliminary X-ray studies of the primitive crystals showed considerable extinction effects, obviously both primary and secondary. Consequently, routine extinction correction was not sufficient for a charge distribution analysis, (*cf.* Downs *et al.* 1985). Therefore, a special thermal treatment was applied to avoid, at least, the primary extinction (Vidal-Valat, Vidal, Zeyen & Kurki-Suonio, 1979; Vidal, Vidal-Valat, Galtier & Kurki-Suonio, 1981; Vidal, Vidal-Valat & Zeyen, 1985; Vidal & Vidal-Valat, 1986). The quenching procedure, described in detail by Vidal *et al.* (1985), resulted in considerable increase of the diffraction intensities, about 40 % in the most extinguished reflections. As a consequence, the extinction corrections as determined by the conventional fitting procedure were reduced to a satisfactory level, (*cf.* Table 2).

Table 1. Basic data and results of the preliminary refinement

Space group	No. 186	$P6_3mc$	
Cell parameters	$a = b = 2.699(3) \text{ \AA}$ $\alpha = \beta = 90^\circ$	$c = 4.385(5) \text{ \AA}$ $\gamma = 120^\circ$	
Atomic positions	$\text{Be}_1 : \frac{1}{3}, \frac{2}{3}, 0$ $\text{O}_1 : \frac{1}{3}, \frac{2}{3}, z$	$\text{Be}_2 : \frac{2}{3}, \frac{1}{3}, \frac{1}{2}$ $\text{O}_2 : \frac{2}{3}, \frac{1}{3}, \frac{1}{2} + z$	$z = 0.3778(4)$
Site symmetry	exact: $3m$	approximate: $4^-3m$	
Matrix of local coordinate axes for $\text{O}_1$ and $\text{Be}_1$	$\begin{bmatrix} 1 & -1 & 0 \\ 1 & 1 & 0 \\ 0 & 0 & 1 \end{bmatrix}$	$\begin{bmatrix} -2 & -1 & -\beta \\ 12 & -\beta \\ 1 & -1 & -\beta \end{bmatrix}$	$\beta = \sqrt{\frac{3}{2}} \frac{a}{c} = 0.75384$
Site symmetric harmonics	exact: real spherical $(n, m, p) = (n, 3\mu, +)$	approximate: even octahedral and odd tetrahedral $n = 0, 3, 4, 6, 7, \dots$	
Atomic factors	$\text{Be}^{2+}$ $\text{O}^{2-}$	International Tables vol. 1V (1974) Sanger (1969)	
Anomalous scattering coefficients for $\text{MoK}_\alpha$	$\text{Be}^{2+}$ $\text{O}^{2-}$	$f' = 0.0$ $f' = 0.008$	$f'' = 0.0$ $f'' = 0.006$ Cromer and Libermann (1970)
Atomic mean-square displacements in $\text{Å}^2$	$\langle u_1^2 \rangle = \langle u_2^2 \rangle$ $\langle u_3^2 \rangle$	$\text{Be}^{2+}$ 0.0041(3)	$\text{O}^{2-}$ 0.0035(1)
spherical average prolateness	$\langle u^2 \rangle = \frac{1}{3} \sum_i \langle u_i^2 \rangle$ $\Delta_1 \langle u^2 \rangle = \langle u_3^2 \rangle - \langle u^2 \rangle$	0.0053(5) 0.0045(3)	0.0036(1) 0.00353(7)
Crystal volume	0.0105 mm <sup>3</sup>		
Linear absorption coefficient $\text{MoK}_\alpha$	1.8 cm <sup>-1</sup>		
Isotropic mosaic spread parameter	$g = 2.0(1) \times 10^{-4} \text{ rad}^{-1}$		

Basic data are reported in Table 1. The sample was a vertical prism with a half hexagon base bounded by  $p$  and  $m$  faces, and with the dimensions 0.40 mm, 0.125 mm and 0.15 mm parallel to  $c$ ,  $b$  and  $a$ , respectively. The crystallographic parameters were obtained through a least-squares refinement based on an X-ray diffraction pattern.

All 101 independent reflections up to  $1.26 \text{ \AA}^{-1}$  in  $\sin\theta/\lambda$  were measured. The intensities in a whole octant were collected at 300 K on a three-circle Enraf-Nonius diffractometer for Mo  $K\alpha$  radiation using a graphite monochromator with  $0.6^\circ$  mosaicity. The technical and geometrical properties of the apparatus have been described by Vidal-Valat *et al.* (1975). A  $\theta$ - $2\theta$  scan with programmed scan and aperture was used to make relevant TDS corrections possible. The dead-time correction was less than 1 % due to the low counting rate.

The effects of multiple scattering were essentially removed by setting the crystallographic and diffractometer axes for each reflection separately to find a position where multiple scattering was not present. Equivalent and forbidden reflections were measured to detect possible residual multiple scattering. The intensities suspected of multiple scattering were remeasured in a tilted setting of the crystal with the  $c$  axis deviating by less than 1 % from the  $\varphi$  axis of the diffractometer. A rotation around the  $c$  axis, reviewing multiple scattering positions, confirmed the absence of multiple scattering in the data. The internal agreement of observed intensities of equivalent reflections was always better than 1 %. The variations were included in the experimental uncertainties  $\delta F_o$  of Table 2.

Background corrections as described by Vidal, Vidal-Valat, Galtier & Kurki-Suonio (1981), Lorentz and polarization corrections, and the absorption correction of Busing & Levy (1957) were applied on the intensities.

The TDS corrections were evaluated with the program of de With, Harkema & Feil (1976) using the elastic constant of Cline, Dunegan & Henderson (1967). These corrections were small, less than 1 % in intensity, owing to the hardness of BeO.

### The preliminary refinement

A preliminary analysis of the entire set of observed intensities was made using the *LINEX* program of Becker & Coppens (1975).

The theoretical model was the conventional rigid spherical-ion model with atomic scattering factors given by *International Tables for X-ray Crystallography* (1974) for  $\text{Be}^{2+}$  and by Sanger (1969) for oxygen  $\text{O}^{2-}$  in MgO. The structure allows one structural parameter  $z$  and four parameters for anisotropic harmonic motion to be varied independently. The scale factor and the extinction parameters were included in the refinement as experimental parameters to be varied simultaneously.

All different combinations of extinction models were tried, isotropic and anisotropic, mosaic-spread and particle-size type, with and without primary extinction. Isotropic mosaic-spread extinction gave a lower  $R$  factor (0.011) than the particle-size extinction (0.012). No significant improvement was obtained by any of the more sophisticated models. Therefore, the extinction corrections were made according to the isotropic mosaic-spread extinction model.

The parameters obtained are listed in Table 1. The thermal parameters are given also in terms of spherical average and prolateness of the thermal ellipsoid as defined by Vidal, Vidal-Valat, Galtier & Kurki-Suonio (1981).

This preliminary analysis yields experimental structure factors  $|F_o|$  on an absolute scale, corrected for isotropic mosaic-spread extinction and for anomalous dispersion, to be used as the basis of the following multipole analysis of the charge density, as well as theoretical structure factors  $|F_c|$  with phases  $\alpha_c$ , which define the reference model of the analysis. These values are given in Table 2 together with the extinction factors  $y$  of each reflection.

The uncertainties  $\delta F$  in Table 2 are the standard errors (of the mean) for each group of three experimental determinations. Thus, they give estimates of random errors but do not include systematic errors.

Table 2. Structure factors

$h$	$k$	$l$	$b = 2(\sin \theta)/\lambda$ ( $\text{\AA}^{-1}$ )	$F_o$	$\alpha_o$	$F_c$	$\alpha_c$	$F_o^o$	$\alpha_o^o$	$\delta F_o$	$\gamma$
1	0	0	0.42783	7.4848	0.50000	7.3469	0.50000	5.65218	0.50000	0.004	0.786
0	0	2	0.45610	11.1753	-0.19185	11.1465	-0.19224	10.44677	-0.24335	0.052	0.629
1	0	1	0.48481	6.6462	0.57476	6.6627	0.57582	8.49954	-0.37280	0.034	0.836
1	0	2	0.62535	4.1946	0.31960	4.1432	0.32053	3.80244	0.25586	0.013	0.946
1	1	0	0.74102	9.0893	-0.00000	9.1976	0.00000	5.98746	0.00000	0.005	0.811
1	0	3	0.80691	6.5705	0.33932	6.7215	0.33867	4.66385	0.38492	0.026	0.899
2	0	0	0.85565	3.9563	0.50000	3.9846	0.50000	2.52493	0.50000	0.020	0.964
1	1	2	0.87013	5.7972	-0.16647	5.8392	-0.16537	5.01828	-0.24632	0.015	0.927
2	0	1	0.88552	3.1995	0.03661	3.0435	0.03599	4.42636	0.12575	0.002	0.980
0	0	4	0.91220	2.3298	0.53285	2.1152	0.52540	4.88317	-0.48441	0.001	0.990
2	0	2	0.96962	2.5664	0.33848	2.5981	0.33791	2.18084	0.25463	0.011	0.986
1	0	4	1.00754	0.9163	0.03100	0.8956	0.02669	2.10507	0.01342	0.009	0.986
2	0	3	1.09554	4.9109	-0.16592	4.8856	-0.16533	3.35496	-0.11793	0.025	0.959
2	1	0	1.13192	3.0482	0.50000	2.9793	0.50000	1.91062	0.50000	0.012	0.985
2	1	1	1.15466	2.2607	0.52381	2.2208	0.52675	3.17914	-0.37411	0.012	0.992
1	1	4	1.17525	1.4774	0.52764	1.4739	0.52739	3.54371	-0.48852	0.015	0.996
1	0	5	1.21787	4.3755	0.17982	4.4394	0.17936	2.94094	0.14050	0.007	0.968
2	1	2	1.22036	2.0741	0.33882	2.0280	0.33990	1.76057	0.25578	0.002	0.993
2	0	4	1.25070	0.6836	0.02680	0.6951	0.02717	1.64824	0.01107	0.007	0.999
3	0	0	1.28348	5.1757	0.00000	5.1939	0.00000	3.20781	0.00000	0.008	0.959
2	1	3	1.32261	3.9847	0.33523	3.9842	0.33535	2.73364	0.38349	0.040	0.976
3	0	2	1.36211	3.6192	-0.16209	3.6070	-0.16224	3.08262	-0.24483	0.013	0.980
0	0	6	1.36830	3.4505	0.18503	3.3320	0.18237	3.17877	0.26372	0.035	0.983
2	0	5	1.42559	3.6711	-0.32200	3.7295	-0.32204	2.51164	-0.36031	0.006	0.979
1	0	6	1.43363	1.4753	-0.31602	1.5840	-0.31603	1.36184	-0.22916	0.015	0.996
2	1	4	1.45374	0.6077	0.02657	0.6484	0.02514	1.39773	0.01151	0.001	0.999
2	2	0	1.48203	4.4133	0.00000	4.4130	0.00000	2.88253	0.00000	0.045	0.972
3	1	0	1.54255	2.1580	0.50000	2.1054	0.50000	1.41877	0.50000	0.011	0.993
2	2	2	1.55063	3.1697	-0.16683	3.1290	-0.16718	2.74883	-0.24363	0.022	0.985
1	1	6	1.55607	2.8666	0.18630	2.9040	0.18785	2.65201	0.26512	0.028	0.937
3	1	1	1.55931	1.6595	0.04234	1.6809	0.04091	2.34068	0.13011	0.009	0.996
3	0	4	1.57462	1.2743	0.52727	1.2825	0.52358	2.66420	-0.48701	0.007	0.998
2	1	5	1.60668	3.1827	0.17654	3.2431	0.17584	2.21322	0.13938	0.013	0.984
3	1	2	1.60856	1.4737	0.33190	1.5008	0.33099	1.28332	0.25433	0.002	0.997
2	0	6	1.61381	1.3410	-0.31165	1.3950	-0.31016	1.25192	-0.23257	0.005	0.997
1	0	7	1.65269	1.6610	-0.03012	1.7632	-0.02621	2.12229	-0.11045	0.008	0.995
3	1	3	1.68746	2.9768	-0.15773	2.9978	-0.15967	2.15363	-0.11328	0.015	0.987
4	0	0	1.71130	1.8762	0.50000	1.8485	0.50000	1.25780	0.50000	0.003	0.995
4	0	1	1.72643	1.5548	0.55276	1.5502	0.55045	2.14109	-0.37056	0.001	0.996
2	2	4	1.74027	1.2125	0.52706	1.3701	0.52158	2.36785	-0.48619	0.006	0.998
4	0	2	1.77104	1.3507	0.32683	1.3407	0.32546	1.19758	0.25721	0.014	0.997
2	1	6	1.77581	1.2192	-0.30457	1.2522	-0.30413	1.15567	-0.23194	0.003	0.998
3	1	4	1.79208	0.6494	0.02677	0.6331	0.02103	1.19342	0.01452	0.007	0.999
2	0	7	1.81121	1.5219	0.46372	1.6258	0.46569	1.92360	0.39005	0.015	0.996
0	0	8	1.82440	3.4606	0.01052	3.2875	0.01577	2.48349	0.01467	0.002	0.984
4	0	3	1.84299	2.5415	0.34527	2.6714	0.34305	1.96165	0.38719	0.027	0.989
3	2	0	1.86485	1.6474	0.50000	1.6451	0.50000	1.13173	0.50000	0.003	0.996
1	0	8	1.87389	1.5565	0.59946	1.5841	0.60085	1.21086	-0.36454	0.008	0.996
3	0	6	1.87605	2.2237	0.19992	2.3457	0.19965	2.13261	0.27074	0.023	0.992
3	2	1	1.87874	1.4677	0.56172	1.4485	0.55898	1.97408	-0.37082	0.015	0.997
3	1	5	1.91823	2.5306	-0.32680	2.5707	-0.32855	1.85258	-0.35927	0.012	0.990
3	2	2	1.91981	1.2062	0.32133	1.2119	0.32026	1.08791	0.25624	0.005	0.998
4	0	4	1.93924	0.7199	0.02413	0.6244	0.01958	1.17786	0.01471	0.007	0.999
2	1	7	1.95693	1.4650	-0.04153	1.5127	-0.04140	1.80849	-0.10693	0.007	0.996
4	1	0	1.96054	3.0467	0.00000	3.0610	0.00000	2.12770	0.00000	0.016	0.986
1	1	8	1.96915	2.9800	0.01361	2.9513	0.01618	2.15000	0.01889	0.015	0.987
3	2	3	1.98638	2.3609	0.34732	2.4042	0.34560	1.79118	0.38659	0.010	0.991

To check the nature of the residual experimental information a set of refinements of the Debye-Waller factors was made using partial data. The cut-off of the data was varied from  $(\sin \theta)/\lambda = 0.7 \text{ \AA}^{-1}$  to  $1.26 \text{ \AA}^{-1}$  of the total data with the scale factor fixed to the value found at  $1.26 \text{ \AA}^{-1}$ . It was found that, with increasing cut-off  $(\sin \theta)/\lambda$ , the thermal parameters smoothly approach their final values and remain essentially stable beyond  $1 \text{ \AA}^{-1}$ . This suggests that the X-ray data do not indicate deviations of the ionic form factors from their theoretical values beyond that limit. Thus, the higher reflexions do not contain any further information on the electronic deformations. They are therefore omitted in the subsequent multipole analysis.

## Multipole analysis

The multipole analysis is based on representation of the crystal charge density in terms of site-symmetric multipole expansions,

$$\rho(\mathbf{r}) = \sum_{nmp} \rho_{nmp}(r) Y_{nmp}(\theta, \varphi), \quad (1)$$

centred at the atomic positions.

The functions  $Y_{nmp}$  form a complete set of site-symmetrized harmonics which can be practically expressed in a symmetry-adapted local coordinate system (Kurki-Suonio, 1977; Kurki-Suonio, Merisalo & Peltonen, 1979; Kara & Kurki-Suonio, 1981; Kurki-Suonio & Sälke, 1985).

If the crystal charge distribution is assumed to be composed of atoms then the charge density of each atom can be represented as the corresponding expansion (1) and the atomic factors are similar expansions in reciprocal space

$$f(S) = \sum_{nmp} f_{nmp}(S) Y_{nmp}(\theta, \varphi), \quad (2)$$

where each term is the Fourier transform of the corresponding term of equation (1).

In the analysis the radial densities  $\rho_{nmp}$  in Eq. (1) and radial scattering factors  $f_{nmp}$  in Eq. (2) are calculated from the series

$$\rho_{nmp}(r) = \frac{4\pi(-i)^n}{VN_{nmp}} \sum_{hkl} F_{hkl}(r) \exp[-2\pi i(hx_0 + ky_0 + lz_0)] \times j_n(2\pi rS) Y_{nmp}(\theta_{hkl}, \varphi_{hkl}), \quad (3)$$

$$f_{nmp}(S) = \frac{16\pi^2 R^3}{VN_{nmp}} \sum_{hkl} F_{hkl}(r) \exp[-2\pi i(hx_0 + ky_0 + lz_0)] \times Y_{nmp}(\theta_{hkl}, \varphi_{hkl}) q_n(2\pi RS, 2\pi RS_{hkl}), \quad (4)$$

where

$$N_{nmp} = \int_{4\pi} [Y_{nmp}(\theta, \varphi)]^2 d\Omega, \quad q_n(x, y) = \frac{xj_{n+1}(x)j_n(y) - yj_{n+1}(y)j_n(x)}{x^2 - y^2}$$

and  $j_n(x)$  are the spherical Bessel functions; or from the corresponding difference series with  $F = F_o - F_c$  instead of  $F_o$ . Application of (3) yields (1), representing the crystal charge density around the centre  $\mathbf{r}_0 = (x_0, y_0, z_0)$ . Application of (4) yields (2), representing the scattering factor of the spherical region of radius  $R$  centred at  $\mathbf{r}_0$ .

Table 1 gives the basic parameters of the analysis. The local coordinate system  $X, Y, Z$  for the atom O1 is shown in Fig. 1. The local axes for Be1 have the same orientation. The basis functions  $Y_{nmp}$  for the atomic site-symmetry  $3m$  with this choice of axes are the real spherical harmonics restricted by the index rule  $(nmp) = (n, 3\mu, +)$ . If series (2) represents O1 or Be1 the corresponding series for O2 or Be2 is

$$f(S) = \sum_{nmp} (-1)^\mu f_{nmp}(S) Y_{nmp}(\theta, \varphi),$$

for the same orientation of axes.

The analysis consists essentially of interpretation of the differences between the data  $F_o$  and the reference model  $F_c$  in terms of multipole expansions. It does not involve any attempts to specify this interpretation in terms of analytical models for the charge density and anharmonic ionic vibrations. Therefore it also does not lead to any parametrized model, the validity of which could be estimated in terms of some goodness-of-fit criterion.

## Phase refinement

This kind of multipole analysis has been applied earlier to centro-symmetric structures only. The non-centrosymmetric space group of BeO brings the phase problem causing additional difficulty in the analysis and a new source of uncertainty in the results.

Calculation of the series (3) and (4) requires knowledge of the structure factors  $F_o$  including the phases  $\alpha_o$ . The theoretical structure factors of the reference model give approximate phases  $\alpha_o \simeq \alpha_c$ , except for weak reflexions. In a charge density analysis this is, however, insufficient. Therefore an iterative procedure was applied to account for the effect of the ionic deformations on the phases.

The phases  $\alpha_c$  were taken as the first approximation of  $\alpha_o$ . The radial functions  $\Delta f_{nmp}$  thus obtained from series (4) represent the ionic deformations in the first approximation and yield the first order correction to the theoretical atomic factors in the form of multipole expansions. The phases of the modified reference model, thus obtained, were adopted as  $\alpha_o$  in the second approximation and new radial functions  $\Delta f_{nmp}$  could be calculated using these  $F_o$  and the original  $F_c$  } to yield phases  $\alpha_o$  in the third approximation. This procedure was repeated iteratively. All low-order components (up to  $n = 6$ ), which in the first step showed significant values, were included in the iteration, i.e.  $(nmp) = (20+)$  for  $\text{Be}^{2+}$  and  $(20+)$ ,  $(30+)$ ,  $(33+)$ ,  $(40+)$ ,  $(60+)$  and  $(66+)$  for  $\text{O}^{2-}$ .

This procedure was found to convergence rapidly. After five cycles of iteration the radial functions  $f_{nmp}$  and, hence, the phases reached stationary values which did not change significantly in further cycles. These phases were then taken as the experimental phases and are given as  $\alpha_o$  in Table 2. The final analysis was based on  $F_o$  thus obtained.

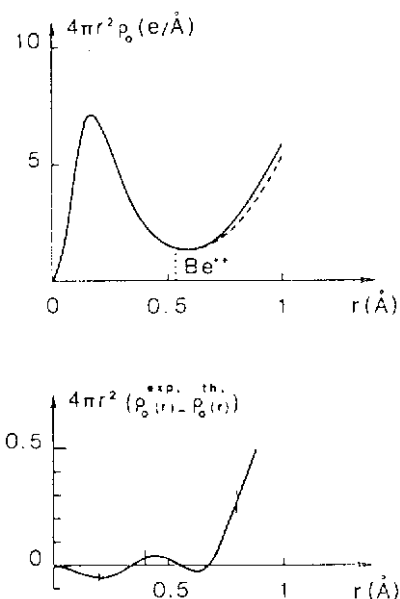
## The course of analysis

Except for the iterative phase refinement, the steps of the analysis are similar to those in case of centrosymmetric structures as described in detail by Vidal, Vidal-Valat, Galtier & Kurki-Suonio (1981) and Kurki-Suonio & Sälke (1984). First the spherical radial densities  $4\pi r^2 \rho_o(r)$  for both ions are calculated from series (3) with  $n = 0$  completed with an asymptotic Gaussian residual term (Sälke & Kurki-Suonio, 1984). The Gaussians used for this purpose were obtained through asymptotic fitting at large  $(\sin \theta)/\lambda$  to the theoretical atomic factors used.

The resulting radial densities around the  $\text{Be}^{2+}$  and  $\text{O}^{2-}$  positions in the crystal are shown in Figs. 2 and 3 together with a comparison with those of the reference model. On the basis of these figures the values  $R_{\text{Be}} = 0.7$  and  $R_{\text{O}} = 1.3$  Å were chosen for the radii of the partitioning spheres needed for calculation of  $\Delta f_{nmp}$  in the iterative phase refinement. These values are slightly larger than the radii of the best separation defined by the minima of these curves.

It should be noted that the effect of this refinement on the experimental curves in these figures is less than the thickness of the curves. The radii assumed on the basis of the unrefined data could therefore be used throughout the iteration.

Fig. 2. Radial charge density around  $\text{Be}^{2+}$  in BeO; — experimental, - - - - theoretical.



The primary discussion of the significance of the different non-spherical components as well as the final conclusions concerning the atomic deformations are based on the radial atomic factors  $\Delta f_{nmp}$  calculated from series (4). The non-spherical radial densities  $\rho_{nmp}$  are mainly used for representation of the results and for demonstration of the concrete significance of the conclusions in real space.

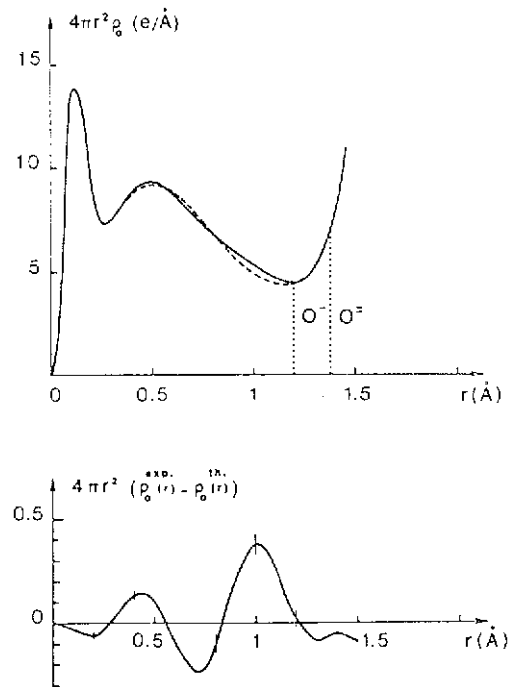


Fig. 3. Radial charge density around  $O^{2-}$  in  $BeO$ ; — experimental, ---- theoretical.

### Subtraction of Beryllium

The beryllium ion  $Be^{2+}$  is small and compact. According to Fig. 2 it is a rather well defined separable entity with all its two electrons within the radius of best separation. The radial scattering factors  $\Delta f_{nmp}$  of Fig. 4 give therefore an exhaustive picture of its deviations from the reference model. The only significant deformation component is  $(20+)$ , the origin of which will be discussed later. There is no evidence of the  $Be1-O2$  bond formation, which would give significant third or fourth order components.

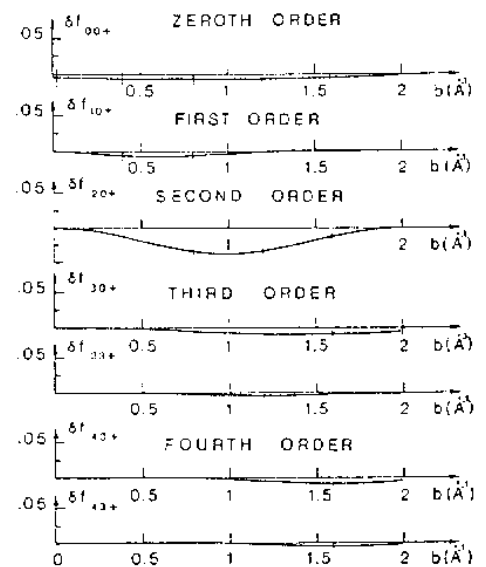


Fig. 4. Radial scattering amplitudes of the multipole components of  $Be^{2+}$ . Radius of partitioning sphere  $R_{Be} = 0.7 \text{ \AA}$ .

For the oxygen ion  $O^{2-}$  quite the opposite is true. As a free ion it is unstable. In a crystal it is stabilized by the presence of the cation lattice. Even then it is large and diffuse. Fig. 3 shows that there are only nine electrons within the radius of best separation. Therefore the spherical partitioning does not yield a full description of its outer electrons. Still there are several significant components up to sixth order.

In order to get a full picture of the multipole expansion of the oxygen ions the contribution of the rather well defined  $Be^{2+}$  ions was subtracted from the structure factors  $F_o$ . This contribution was taken as that of the theoretical ions of the reference model modified with the only significant component  $\Delta f_{20+}$  obtained. The resulting "experimental structure factors  $F_o^O$  of the  $O^{2-}$  lattice" are listed in Table 2. The final results on  $O^{2-}$  are based on these structure factors and on their comparison with a reference model with  $O^{2-}$  contribution only.



Fig. 5 presents the radial charge density  $4\pi r^2 \rho_0$  around the  $O^{2-}$  position in this  $O^2$  lattice of BeO and a comparison with that of the reference model. It is clear from this figure that we can now get a satisfactory description of the whole  $O^{2-}$  ion by using the partitioning sphere of radius  $R_O = 1.46 \text{ \AA}$ , which contains the total of ten electrons. The resulting radial atomic factors  $\Delta f_{nmp}^f$  are given in Fig. 6.

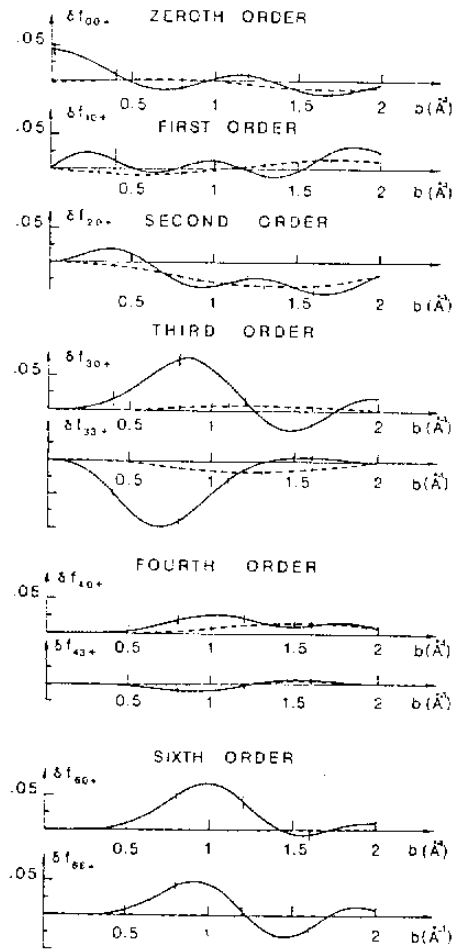


Fig. 5. Radial charge density around  $O^{2-}$  in BeO after subtraction of  $Be^{2+}$ ; — experimental, ---- theoretical.

### Discussion of results

When discussing the nature and significance of different multipole components it must be taken into account that:

the error bars given in Figs. 5 and 6 are based on statistical accuracy only and do not account for any systematic errors;

the smallness of high-order components is a qualitative argument for internal consistency of the data;

the multipole components describe the integral three-dimensional behaviour with the angular dependence defined by the well-known symmetrized harmonics  $Y_{nmp}(\theta, \varphi)$ ;

the radial scattering factors  $\Delta f_{nmp}^f$  represent the information in reciprocal space and their values at  $(\sin \theta)/\lambda$  below the experimental cut-off are therefore not sensitive to cut-off errors (Kurki-Suonio, 1968);

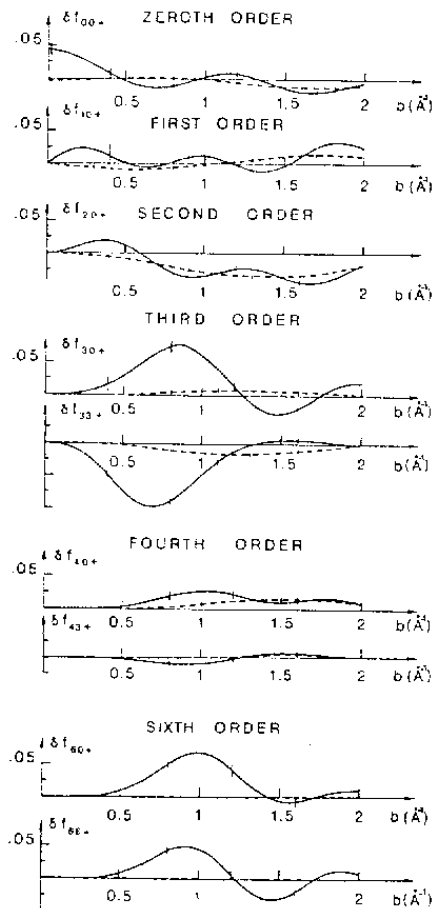


Fig. 6. Radial scattering amplitudes of the multipole components of  $O^{2-}$  in BeO after subtraction of  $Be^{2+}$  with two different radii  $R_O$  of the partitioning sphere; —  $R_O = 1.46 \text{ \AA}$ , ----  $R_O = 0.7 \text{ \AA}$ .

owing to the reciprocity theorem, features at small  $(\sin \theta)/\lambda$  correspond to outer effects and are thus likely to be of electronic origin, while broad features extending to large  $(\sin \theta)/\lambda$  correspond to core effects and are thus likely to be of dynamical origin; and the Fourier-Bessel transformation relating the radial densities to radial scattering factors transforms a smooth function  $\rho_{nmp}(\mathbf{r})$  with one single peak into a smooth function  $f_{nmp}$  of similar kind multiplied by the phase factor  $i^n$ .

### (1) Beryllium

According to Figs. 2 and 4 the deviations of the beryllium ion from the reference model can be exclusively represented by a quadrupole-like (20+) component. Its low- $(\sin \theta)/\lambda$  nature suggests electronic origin. It clearly cannot be explained by additional prolateness of the harmonic motion. It is, however, possible that a strong anharmonicity of vibrations particularly in the  $c$  direction, together with the anisotropic Debye-Waller factor fitted to suppress the curve to zero at large  $(\sin \theta)/\lambda$ , could give rise to a similar feature. The independence of the Debye-Waller factors of the cut-off beyond  $(\sin \theta)/\lambda = 1 \text{ \AA}^{-1}$ , confirmed in the preliminary refinement, however, makes this alternative less probable as the sole explanation.

The (20+) component can, thus, be interpreted dominantly as a bonding feature with a possibility of some anharmonicity effect superimposed. It indicates angular charge transfer from the  $XY$  plane to the direction of  $Z$  axis. According to this nature it would be a sign of Be1–O1 bonding or rather, because of its symmetry, a sign of some electronic bridging between the two successive oxygen planes. In terms of electron counts it is a weak effect, involving a total of  $0.026 \pm 0.003$  electrons transferred, as obtained by integration of the corresponding radial density  $r^2\rho_{20+}(\mathbf{r})$ . It should be noted that there is no indication in the  $\text{Be}^{2+}$  ion of formation of directional Be1–O2 bonding which would give rise to significant third order components.

### (2) Oxygen

According to Fig. 5 the  $\text{O}^{2-}$  ion is on the average slightly compressed in its outer parts compared with the reference model. The radial scattering factors of Fig. 6 show in addition several significant non-spherical features. They indicate both electronic or bonding and dynamical or anharmonicity effects. This can be demonstrated by diminishing the partitioning sphere sufficiently to exclude the bonding effects.

The dashed lines give the radial scattering factors corresponding to  $R_{\text{O}} = 0.7 \text{ \AA}$ . When one takes into account the small size of the sphere, several of the remaining features are significant or almost significant and can be interpreted mainly as indications of anharmonic motion. The most prominent feature is an even anharmonicity in the  $Z$  direction. Both (20+) and (40+) indicate that the vibrational smearing function is more prolate and hence the one-particle potential in the  $Z$  direction is softer than allowed by a harmonic model. A suspicion of asymmetry of these vibrations is seen in (10+), which would mean that the potential is slightly softer opposite to the O1–Be1 bond direction. The component (33+) indicates also the possibility of an odd anharmonicity perpendicular to the  $Z$  axis with some softening in the local  $X$ -axis and symmetry-related directions.

The indications of bonding effects are strong in (30+), (33+), (60+) and (66+) and weak but probably significant in (40+). A dipole-like deformation (10+), if any, is too weak to be detectable. The quadrupole deformation (20+) is obscured by the anharmonicity effects.

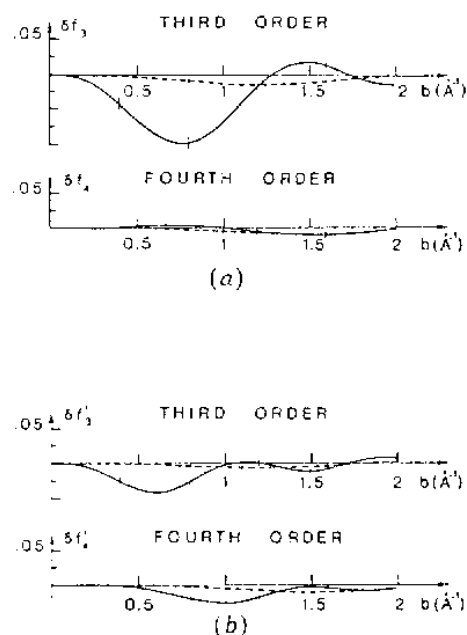
The arrangement of the neighbouring  $\text{Be}^{2+}$  ions is very close to tetrahedral, *cf.* Fig. 1. The difference of the two bond lengths,  $1.648 \text{ \AA}$  and  $1.657 \text{ \AA}$  for O1–Be2 and O1–Be1, respectively, is small and the angle between the bonds is  $109, 0^\circ$  compared with the ideal  $109, 47^\circ$ . It would be natural to assume that the bonding deformations follow closely the approximate tetrahedral symmetry.

The degree to which this is realized can be checked by a calculation of the multipole components in the other local coordinate system  $X', Y', Z'$  of Fig. 1 defined by a matrix given in Table 1. It is adapted to this approximate symmetry so that, in this system, the neighbouring Be1 lies in the 111 direction and the three Be2 neighbour deviate similarly from their ideal positions in

the directions  $1\bar{1}\bar{1}$ ,  $\bar{1}1\bar{1}$ ,  $\bar{1}\bar{1}1$ . An exactly tetrahedral bonding would now yield only cubic harmonic components.

As shown by Fig. 7 there is in the third order a dominant cubic harmonic component, which alone would indicate similar concentration of charge distribution in all four bond directions. The non-cubic multipole (30+) orthogonal to the cubic one is, however, significant. It indicates considerable asymmetry between the two kinds of bonds. It reduces the charge density in the O1–Be1 bond and turns the O1–Be2 bond towards the *XY* plane. The fourth order is concentrated exclusively to the non-cubic multipole (42+) orthogonal to the cubic harmonics. As a result the violation of the approximate tetrahedral symmetry is very strong.

Fig. 7. Radial scattering amplitudes of the multipole components of  $O^{2-}$  in the coordinate system adapted to the approximate tetrahedral symmetry after subtraction of  $Be^{2+}$ : (a) cubic harmonic components, (b) components orthogonal to the cubic harmonics; —  $R_0 = 1.46 \text{ \AA}$ , - - -  $R_0 = 0.7 \text{ \AA}$ .



It is concluded that these bonding effects cannot be regarded as signs of directional O–Be bonds, particularly since they have no counterparts in the  $Be^{2+}$  ions. Rather they indicate bonding between the oxygen ions in the hexagonal  $O^{2-}$  plane, i.e. formation of O1–O1 and O2–O2 bonds.

### (3) Illustration in real space

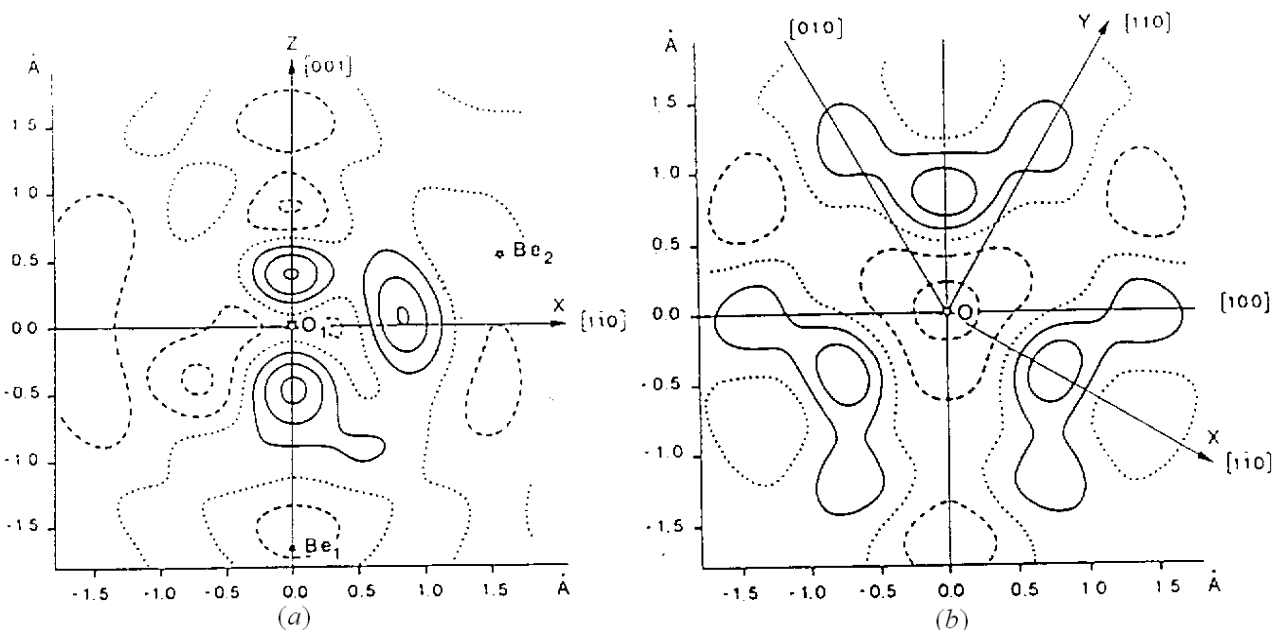


Fig. 8. Difference density corresponding to the multipole expansion centred at O1 in BeO with all significant components up to sixth order in (a) the XZ plane, (b) the XY plane of the local coordinate system. Contour interval  $0.05 e \text{ \AA}^{-3}$ , solid line positive, dashed line negative and dotted line zero.

Figs. 8–10 demonstrate in real space the nature of the statements based on radial scattering factors. Figs. 8(a), (b) represent the difference charge density corresponding to the multipole expansion of oxygen up to sixth order in the XZ and XY planes, respectively. Figs. 9(a), (b) show for comparison the difference Fourier maps of the  $O^{2-}$  lattice corresponding to the  $Be^{2+}$ -subtracted data, while Fig. 10 is the difference Fourier map of the XZ plane before subtraction.

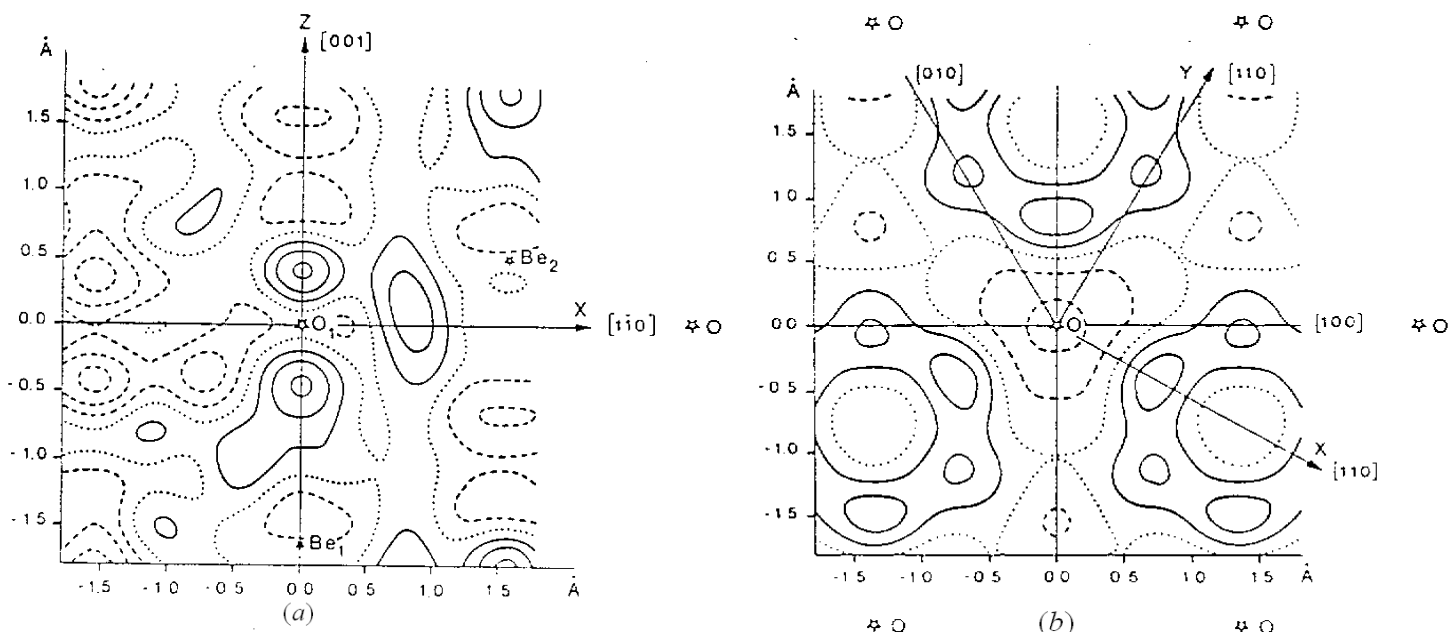
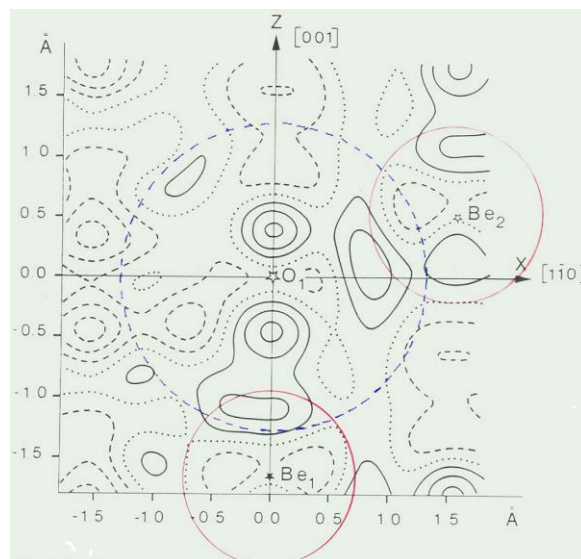


Fig. 9. Difference density in (a) the XZ plane, (b) the XY plane of the local coordinate system centred at O1 in BeO after subtraction of the  $\text{Be}^{2+}$  ion.

To suppress the effects of anharmonicity the series have been terminated at  $(\sin \theta)/\lambda = 0.7 \text{ \AA}^{-1}$ . Still the peaks close to the centre on the Z axis correspond to what has been interpreted as anharmonicity effects. The peak towards Be2 in the XZ plane in Fig. 8(a) is a section of one of the three positive lobes in Fig. 8(b). In the Fourier map Fig. 9(b) the ring-like features are formed by superposition of these lobes of the three O1 ions lying symmetrically with respect to the Be2 ion slightly above. In Fig. 10 a section of the quadrupole like deformation of the  $\text{Be}^{2+}$  ion is clearly visible. These are the most prominent features of what has been called bonding effects in the above.

Fig. 10. Difference density in the XZ plane of the local coordinate system centred at O1 in BeO before subtraction of the  $\text{Be}^{2+}$  ion.



Comparison of the Fourier maps, Figs. 9 and 10, with the multipole maps, Figs. 8(a) and (b), in the light of the conclusions made above demonstrates also the difference between the map and multipole representations, (Figs. 2–7), as well as the advantages achieved in basing the conclusions on the multipoles, (*cf.* Kurki-Suonio & Sälke 1984). While the maps give a picture of the electron distribution in two dimensional slices showing sections of all details on a similar basis without any reference to their origin or significance, the multipole representation builds a view of three-dimensional pieces, each showing the coherent three-dimensional behaviour of the charge density of one atom. Only on the basis of the multipole representation is it possible to assign the details of the Fourier maps to different atoms as part of their three-dimensional integral behaviour. For instance, the second peak between the central O1 and Be1 in Fig. 10 lies within the partitioning spheres of both ions but it is uniquely assigned as a part of the (20+) deformation of Be1. At the same time the multipole representation damps effectively the noise of the data and draws, thus, the attention to the significant features only.

The picture thus created of BeO corresponds to a structure built of alternating hexagonal O1 and O2 plane nets. There is a considerable amount of bonding charge bridging the oxygen ions of each plane. The O1–O1 and O2–O2 bonds formed in this way are strongly bent towards the  $\text{Be}^{2+}$

ions lying above the plane. Fig. 4 shows that the spherical partitioning made includes 10 electrons per oxygen ion. Thus, this description already involves all the electrons of the  $O^{2-}$  lattice. Particularly, there is none left to build up any bonding density between the layers. The bonding between the  $O^{2-}$  planes seems to be established by the  $Be^{2+}$  ions embedded in the  $O^{2-}$  lattice with their charge distributions slightly deformed like trying to build bridges between the  $O^{2-}$  layers.

#### (4) *Reliability*

Many kinds of cross checks were made repeatedly throughout the calculations to ensure that the methods applied do not produce artefacts in the results. The effect of each of the parameters of the reference model was confirmed to be on the relevant multipole component only,  $z$  on (10+) of oxygen, spherical average  $\langle u^2 \rangle$  and prolateness  $\Delta_1 u^2$  of the thermal parameters of beryllium and oxygen on (00+) and (20+) of the respective ion. The other components were completely insensitive to them (Kurki-Suonio & Sälke, 1984). These parameters thus cause no uncertainties other than those already discussed. The effects caused by the spherical volume partitioning are well-known (Kurki-Suonio, 1968).

Special attention was paid to possible large errors in some single structure factors. Calculations of the entire set of radial scattering amplitudes were performed with several of the largest  $\Delta F$ . It was confirmed that none of the significant components could be created by single reflexions but that all the features discussed are due to coherent systematics inherent in a large number of structure factors.

The least known factor in the present analysis is the iterative phase refinement introduced. The convergence shows that the "experimental phases" obtained make the experimental data consistent with the significant multipole components, while the theoretical phases do not. The iteration changes the radial atomic factors essentially from their unrefined values and is thus important. It more than doubles the (30+) component of oxygen, strengthens (20+) of beryllium and weakens (20+) and (40+) of oxygen roughly by 20 %, but it does not change the general picture of the significance of the different components. The results vary slightly, by about 5 % at most of the significant components, depending on components included in the refinement. The most important components to be included are clearly the third order components of oxygen. These variations can be assumed to give a measure of the uniqueness of the procedure.

#### (5) *The alkaline-earth series*

Comparison of the results on other alkaline-earth oxides (Vidal-Valat, Vidal & Kurki-Suonio, 1978) shows a systematic variation in the nature of the oxygen ion. It is best reflected in the radial charge densities ( $4\pi r^2 \rho_0$ ) at the radius of best separation which is a qualitative indication of the separability of oxygen from its surroundings. It has the values 1.2, 1.2, 2.3, 2.8 and  $4.46 e \text{ \AA}^{-1}$  for BaO, SrO, CaO, MgO and BeO, respectively. Even in the  $O^{2-}$  lattice of BeO it is as high as  $3.80 e \text{ \AA}^{-1}$ . These values can be understood to indicate decreasing ionicity of  $O^{2-}$  in the row from the heavier to the lighter compounds, its outer electrons becoming more and more diffuse. Still, in all the cubic compounds oxygen can be described as a separable  $O^{2-}$  entity with different degrees of deformation. It is only in BeO that the deformations are strong and concentrated enough to create density bridges as an indication of covalency. This qualitative change in the nature of the electronic deformations is also clear in the radial atomic factors where as high as sixth-order multipoles are needed to describe the bonding effects in BeO.

The financial support of CNRS which has made this international co-operation possible is gratefully acknowledged.

## References

- BECKER, P. J. & COPPENS, P. (1975). *Acta Cryst.* **A31**, 417–425.
- BUSING, W. R. & LEVY, H. A. (1957). *Acta Cryst.* **10**, 180–187.
- CAMPBELL, I. E. (1956). *High-Temperature Technology*. Electrochemical Society. New York: John Wiley & Sons.
- CHITRA, S., VEMPATI, C. S. & JACOBS, P. W. (1983). *Cryst. Lattice Defects Amorphous Mat.* **10**, 9–17.
- CLINE, C. F., DUNEGAN, H. L. & HENDERSON, G. W. (1967). *J. Appl. Phys.* **38**, 1944–1948.
- CROMER, D. T. & LIBERMAN, D. (1970). *J. Chem. Phys.* **53**, 1891–1898.
- DOWNS, J. W., ROSS, F. K. & GIBBS, G. V. (1985). *Acta Cryst.* **B41**, 425–431.
- FUKAMACHI, T. & HOSOYA, S. (1970). 1. *Phys. Soc. Jpn.* **28**, 161–167.
- HASHIMOTO, M. & SANTRY, D. P. (1978). *Theor. Chim. Acta*, **50**, 39–48.
- HEWAT, A. (1972). *J. Phys. C*, **5**, 1309–1316.
- HUGGINS, M. L. & SAKAMOTO, Y. (1957). *J. Phys. Soc. Jpn.* **12**, 241–251.
- International Tables for X-ray Crystallography* (1974). Vol. IV.  
Birmingham: Kynoch Press. (Present distributor D. Reidel, Dordrecht, The Netherlands.)
- JEFFREY, G. A., PARRY, G. S. & MOZZI, R. L. (1956). *J. Chem. Phys.* **25**, 1024–1031.
- JULG, A. (1978). *Phys. Chem. Miner.* **3**, 45–53.
- KARA, M. & KURKI-SUONIO, K. (1981). *Acta Cryst.* **A37**, 201–210.
- KINGERY, W. D., FRANCH, J., COBLE, R. L. & VASILOS, T. (1954). *J. Am. Ceram. Soc.* **37**, 2, 107.
- KURKI-SUONIO, K. (1968). *Acta Cryst.* **A24**, 379–390.
- KURKI-SUONIO, K. (1977). *Isr. J. Chem.* **16**, 115–123, 132–136.
- KURKI-SUONIO, K., MERISALO, M. & PELTONEN, H. (1979). *Phys. Scr.* **19**, 57–63.
- KURKI-SUONIO, K. & SÄLKE, R. (1984). *Local Density Approximations in Quantum Chemistry and Solid State Physics*, edited by J. P. DAHL & J. AVERY, pp. 713–733. New York and London: Plenum Press.
- KURKI-SUONIO, K. & SÄLKE, R. (1985). Report Series in Physics, HU-P-240, Univ. of Helsinki, Finland.
- MAIR, S. L. & BARNEA, Z. (1975). *Acta Cryst.* **A31**, 201–207.
- MIURA, M., MURATA, H. & SHIRO, Y. (1977). *J. Phys. Chem. Solids*, **38**, 1071–1073.
- MIURA, M., MURATA, H. & SHIRO, Y. (1978). *J. Phys. Chem. Solids*, **39**, 669–673.
- MIURA, M., SATO, T., MURATA, H. & SHIRO, Y. (1980). *J. Phys. Chem. Solids*, **41**, 189–197.
- MOSS, G. & BARN EA, Z. (1976). *J. Appl. Cryst.* **9**, 510–511.
- MUCILLO, R. & BLACK, A. R. (1980). *Int. Symp. on Electrets and Dielectrics*, Sao Carlos, Brazil, 1–6 September 1975, pp. 357–364. Rio de Janeiro: Academia Brasileira de Ciencias.
- NUSIMOVICI, A. (1968). Thesis, Univ. of Paris, France.
- PRYOR, A. W. & SABINE, T. M. (1964). *J. Nucl. Mater.* **14**, 275–281.
- RANI, N., GUPTA, D. K. & GUPTA, H. C. (1981). *Int. J. Pure Appl. Phys.* **19**, 316–318.
- SABINE, T. M. & DAWSON, B. (1963). *Int. Conf. on Beryllium Oxide*, Newport, Sydney, Australia, 21–25 October 1963.
- SABINE, T. M. & HOGG, S. (1969). *Acta Cryst.* **B25**, 2254–2256.
- SÄLKE, R. & KURKI-SUONIO, K. (1984). Report Series in Physics, HU-P-233, Univ. of Helsinki, Finland.
- SANGER, P. L. (1969). *Acta Cryst.* **A25**, 694–702.
- SMITH, D. K., NEWKIRK, H. W. & KAHN, J. S. (1964). *J. Electrochem. Soc.* **111**, 78–87.
- VIDAL, J. P. & VIDAL-VALAT, G. (1986). *Acta Cryst.* **B42**, 131–137.
- VIDAL, J. P., VIDAL-VALAT, G., GALTIER, M. & KURKI-SUONIO, K. (1981). *Acta Cryst.* **A37**, 826–837.
- VIDAL, J. P., VIDAL-VALAT, G., GALTIER, M. & KURKI-SUONIO, K. (1982).  
*Sagamore VII Conf. on Charge, Spin and Momentum Densities*, Nikko, Japan. Abstr. p. 26.
- VIDAL, J. P., VIDAL-VALAT, G. & ZEYEN, C. M. E. (1985). *Nucl. Instrum. Methods*, **228**, 569–575.
- VIDAL-VALAT, G., VIDAL, J. P. & KURKI-SUONIO, K. (1975).  
Report Series in Physics, No. 107, Univ. of Helsinki, Finland.
- VIDAL-VALAT, G., VIDAL, J. P. & KURKI-SUONIO, K. (1978). *Acta Cryst.* **A34**, 594–602.
- VIDAL-VALAT, G., VIDAL, J. P., ZEYEN, C. M. E. & KURKI-SUONIO, K. (1979). *Acta Cryst.* **B35**, 1584–1590.
- WHITELEY, B., MOSS, G. & BARNEA, Z. (1977). *Phys. Lett. A*, **60**, 429–439.
- WHITELEY, B., MOSS, G. & BARNEA, Z. (1978). *Acta Cryst.* **A34**, 130–136.
- WITH, G. DE, HARKEMA, S. & FEIL, D. (1976). *Acta Cryst.* **B32**, 3178–3184.